Accepted by ApJ Letters
Preprint typeset using LaTeX style emulateapj v. 04/03/99

arXiv:astro-ph/0008243v1 16 Aug 2000

MAGNETIC FIELDS AND THE TRIAXIALITY OF MOLECULAR CLOUD CORES

Shantanu Basu
Department of Physics and Astronomy, University of Western Ontario, London, Ontario N6A 3K7, Canada;
basu@astro.uwo.ca
Accepted by ApJ Letters

ABSTRACT

We make the hypothesis that molecular cloud fragments are triaxial bodies with a large scale magnetic field oriented along the short axis. While consistent with theoretical expectations, this idea is supported by magnetic field strength data, which show strong evidence for flattening along the direction of the mean magnetic field. It is also consistent with early submillimeter polarization data, which show that the projected direction of the magnetic field is often slightly misaligned with the projected minor axis of a molecular cloud core, i.e., the offset angle Ψ is nonzero. We calculate distributions of Ψ for various triaxial bodies, when viewed from a random set of viewing angles. The highest viewing probability always corresponds to $\Psi = 0^\circ$, but there is a finite probability of viewing all nonzero Ψ, including even $\Psi = 90^\circ$; the average offset typically falls in the range $10^\circ - 30^\circ$ for triaxial bodies most likely to satisfy observational and theoretical constraints.
Subject headings: ISM: clouds - ISM: magnetic fields - MHD - polarization

1. INTRODUCTION

Observations establish that magnetic fields play an important role in shaping the structure and dynamics of molecular clouds. Polarization maps reveal that there is a magnetic field threading molecular clouds that is ordered over large scales (e.g., Vrba, Strom, & Strom 1976; Goodman et al. 1990; Schleuning 1998) and Zeeman measurements establish that measured field strengths are invariably strong enough to yield a mass-to-flux ratio very close to the critical value (Crutcher 1999; hereafter C99), i.e., the magnetic energy approximately equals the gravitational binding energy. A problem with absorption maps of the polarization of background starlight is that the densest regions (the cloud cores) are not sampled (Goodman et al. 1995). However, new maps of polarized submillimeter emission (Matthews & Wilson 2000; Ward-Thompson et al. 2000) do sample these regions and provide a crucial test of theoretical scenarios involving magnetic fields; in particular, the relative alignment of the projected magnetic field with the projected minor axis of the core density distribution is an important diagnostic.

When making the above comparison, two important factors must be kept in mind: 1) the measured relative alignment is only between two projected quantities in the plane of the sky, and care must be taken to draw inferences about the relative orientation in the actual three dimensional object, and 2) theoretical models of magnetically dominated clouds (e.g., Mouschovias 1976; Lizano & Shu 1989; Fiedler & Mouschovias 1993), while predicting the important effect of flattening along the mean magnetic field direction, are usually restricted (for numerical convenience) to the physically unnecessary assumption of axisymmetry. In fact, it has been known for a long time (Mestel 1965; Lin, Mestel, & Shu 1965) that gravity amplifies anisotropic structure, so that an initially unstable fragment will first collapse along one dimension, forming a sheet, which will subsequently break into elongated filamentary structures. The presence of a large scale magnetic field can enhance this effect, as the first stage of collapse is preferentially along the mean field direction. The subsequent contraction lateral to the field will occur in qualitatively the same manner as described by Mestel (1965), particularly if the cloud is magnetically supercritical, but even if it is subcritical, since the evolution is still driven by gravity (Mouschovias 1978; Langer 1978), but on the ambipolar diffusion (rather than free-fall) time scale. Thus, the most general formation mechanism for a dense core in the magnetic field scenario yields an object flattened along the mean field direction and also having an elongated structure in the lateral direction; such an object is triaxial.

The properties of the projected shapes of triaxial bodies have been investigated in the context of galaxy studies. Stark (1977) has proven the important result that the isocontours of a triaxial body seen in projection are elliptical. Binney (1985) has extended this analysis, and his results can be applied to find the distribution of angular offsets Ψ between the projected field direction and the projected minor axis of a triaxial body, given that the body is primarily flattened along the direction of the mean magnetic field.

In § 2, we review observational evidence to establish that molecular cloud fragments are ubiquitously flattened along the mean magnetic field direction, and in § 3 calculate the distribution of Ψ for various triaxial bodies. In § 4 we discuss how the results relate to current observations and to other theoretical scenarios presented in the literature.

2. CLOUD FLATTENING ALONG MAGNETIC FIELD LINES

The magnetic field strength data of C99 also reveals that the correlation of the line-of-sight field strength $B_{\rm los}$ with the density ρ is in apparent agreement with models of preferential flattening along the magnetic field ($B \propto \rho^{1/2}$; Mouschovias 1976) rather than isotropic contraction ($B \propto \rho^{2/3}$). Figure 1a (equivalent to Fig. 1 of C99) plots (in logarithmic form) the confirmed magnetic field strength detections of C99 against the measured number densities n. The solid line is the least squares best fit, with slope

0.47 ± 0.08, and chi-squared error statistic $\chi^2 = 2.36$. The correlation coefficient is 0.84.

We seek an even better correlation for the C99 data as follows. Consider a cloud that is flattened along the mean magnetic field direction. In this direction, force balance between an isotropic pressure and self-gravity yields

$$\rho_0 \, \sigma_v^2 = \frac{\pi}{2} G \, \Sigma^2, \tag{1}$$

where ρ_0 is the density at the midplane, σ_v is the total (thermal and non-thermal) one-dimensional velocity dispersion, Σ is the column density of the cloud, and G is the gravitational constant. Here we assume that the effect of an external confining pressure is negligible. Furthermore, the relation

$$\frac{\Sigma}{B} \equiv \mu \, (2\pi G^{1/2})^{-1} \tag{2}$$

defines the dimensionless ratio μ of the mass-to-flux ratio to the critical value $(2\pi G^{1/2})^{-1}$ for a disk (Nakano & Nakamura 1978). Combining equations (1) and (2) yields

$$B = (8\pi c_1)^{1/2} \, \frac{\sigma_v \rho^{1/2}}{\mu} \tag{3}$$

(see Mouschovias 1991 for a similar relation), where c_1 ($\gtrsim 1$) is an undetermined proportionality constant between ρ_0 and the mean density ρ. Clearly, the correlation in Figure 1a is imperfect because variations in σ_v and μ are unaccounted for, and the observed quantity $B_{\rm los} = B \cos\theta$ (where θ is the angle between the field direction and the line of sight) does not correspond exactly to B. We improve the correlation by accounting for variations in the observable quantity σ_v. Figure 1b plots $B_{\rm los}$ versus $\sigma_v \, n^{1/2}$ in logarithmic form; equation (3) predicts a slope of 1 to the extent that μ is constant from cloud to cloud. We use values of $\Delta v = \sigma_v (8 \ln 2)^{1/2}$ listed in Table 1 of C99. The correlation coefficient in this plot is 0.95. The solid line is the best least squares fit and has slope 1.00 ± 0.09, and $\chi^2 = 0.79$. The dashed line is the theoretical relation (3) for $\sqrt{c_1}/\mu = 1$. The two lines coincide if $\sqrt{c_1}/\mu = 0.8$. This exceptional correlation leads us to the conclusion that clouds (and cloud fragments) are flattened (at least moderately) along the magnetic field direction, even in the presence of turbulent motions, due to the dynamically important roles of self-gravity and the mean magnetic field. We note that the correlation found in Figure 1b is equivalent to that presented by Myers & Goodman (1988) in their Figure 1 (see also Mouschovias & Psaltis 1995) based on earlier magnetic field data. We also note that our fit to the magnetic field data is quite general; it does not require axisymmetry, or that the Alfvén speed $v_A = B/(4\pi\rho)^{1/2}$ be constant from one cloud to another. However, equation (3) implies that $\sigma_v / v_A = (2c_1)^{-1/2} \mu$, so that the Alfvén mach number may be approximately constant, if non-thermal motions dominate thermal motions and μ does not vary much from one cloud to another.

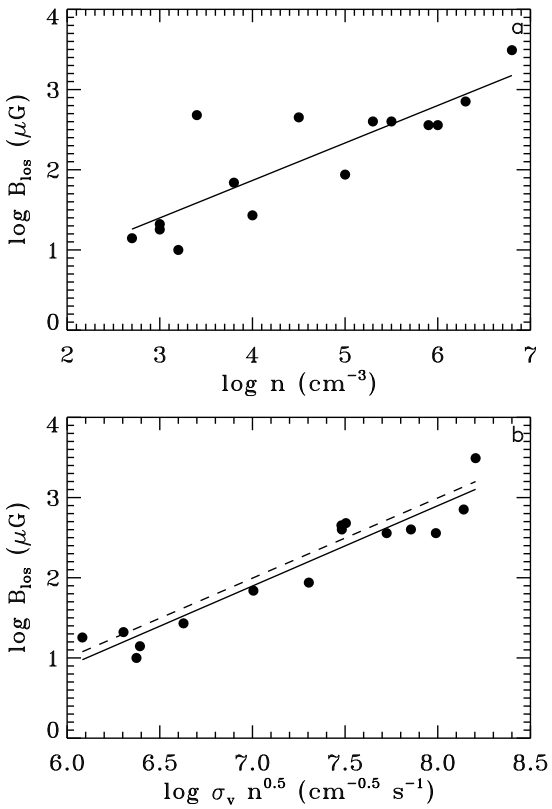

Fig. 1 a) Plot of $\log B_{\rm los}$ versus $\log n$ from the C99 data set. The solid line is the best fit (see text). The correlation coefficient is 0.84. b) Plot of $\log B_{\rm los}$ versus $\log \sigma_v n^{1/2}$ for the same data. The correlation coefficient is 0.95. The solid line is the best fit, and the dashed line is a theoretical relation (eq. [3] for $\sqrt{c_1}/\mu = 1$).

3. PROJECTION OF TRIAXIAL BODIES

Let z be the direction of the mean magnetic field. Since the mean field contributes cloud support against gravity only in the lateral (x and y) directions, but the cloud need not be axisymmetric in the $x-y$ plane, the most general cloud configuration is a triaxial body with the shortest dimension along the $z-$axis. The simplest mathematical description of such a body is

$$x^2 + \frac{y^2}{\zeta^2} + \frac{z^2}{\xi^2} = a^2, \tag{4}$$

where a is a constant, and $1 \geq \zeta \geq \xi$. Here we follow the geometric analysis of Binney (1985) to calculate projected quantities when the object is viewed from an observing angle (θ, ϕ) (where the angles are defined on an imaginary viewing sphere and have their usual meaning in a spherical coordinate system). Defining the quantities

$$A \equiv \frac{\cos^2\theta}{\xi^2} \left(\sin^2\phi + \frac{\cos^2\phi}{\zeta^2} \right) + \frac{\sin^2\theta}{\zeta^2}, \tag{5}$$

$$B \equiv \cos\theta \sin 2\phi \left(1 - \frac{1}{\zeta^2} \right) \frac{1}{\xi^2}, \tag{6}$$

and

$$C \equiv \left(\frac{\sin^2\phi}{\zeta^2} + \cos^2\phi \right) \frac{1}{\xi^2}, \tag{7}$$

it can be shown that the projection in the sky of the triaxial body is an elliptical body of apparent axial ratio

$$q = \left(\frac{A + C - D}{A + C + D} \right)^{1/2}, \quad (8)$$

where $D \equiv \sqrt{(A-C)^2 + B^2}$. Furthermore, the quantity

$$\psi = \frac{1}{2} \arctan \left(\frac{B}{A - C} \right) \quad (9)$$

can be used to find the absolute value of the angular offset between the projected z axis and the apparent minor axis of the projected ellipse. Letting $p = (A - C) \cos 2\psi + B \sin 2\psi$, the required positive definite angle is

$$\Psi = \begin{cases} |\psi| & \text{for } p \leq 0 \\ \pi/2 - |\psi| & \text{for } p > 0. \end{cases} \quad (10)$$

Since Ψ corresponds to the offset between the projected magnetic field $B_\perp$ and the projected minor axis of a core, we calculate the distribution of observed offsets Ψ using a Monte Carlo simulation. A large number $N = 10^6$ of randomly oriented viewing angles (θ, ϕ) are used to generate a distribution of Ψ for a given set of intrinsic axial ratios ζ and ξ of a triaxial body. Figure 2 shows, for each of three cases $\xi = 0.1, 0.3$, and 0.5, the probability distribution function f versus Ψ for three different values of ζ, as well as the dependence of the mean value $\langle \Psi \rangle$ of the distribution and the mean axial ratio $\langle q \rangle$ on ζ. The lower limit of $\zeta = \xi$ corresponds to a prolate object and the upper limit $\zeta = 0.9$ is very nearly an oblate object.

Our calculated distributions show the robust result that there is always a peak in f at $\Psi = 0$, so that it is the most probable value, but that there is a long tail towards all nonzero angles, including $\Psi = 90^\circ$. Figures 2b, 2d, and 2f show how $\langle \Psi \rangle$ varies for clouds of different triaxial ratios; it becomes smaller as a cloud goes toward the oblate limit. For a perfectly oblate cloud ($\zeta = 1$), there would be no distribution, as all viewing angles yield $\Psi = 0$. The distributions for prolate clouds ($\zeta = \xi$)[1] have the largest possible values for $\langle \Psi \rangle$. The values of $\langle q \rangle$ illustrate which triaxial models may be most likely. The crosses highlight the values of ζ for which $\langle q \rangle$ is in the range $0.5 - 0.65$ that is consistent with observations of dense cores (e.g., Myers et al. 1991; Jijina, Myers, & Adams 1999).

While data sets that measure q and Ψ for a large number of cores will ultimately settle the values (and distributions) of ζ and ξ, we do not currently favor highly flattened cases $\xi \approx 0.1$ due to 1) the observational result that highly elongated cores are rarely observed, and 2) the theoretical result that flattening along the magnetic field yields cores of axial ratio $\approx 0.25 - 0.33$ (see Ciolek & Basu 2000 and references therein). Hence, the $\xi = 0.3$ curves represent likely scenarios, although the $\xi = 0.5$ curves cannot be ruled out observationally. The observational constraint on $\langle q \rangle$ also allows the widest plausible range of ζ values when $\xi = 0.3$, rather than imply near-oblate (for $\xi = 0.1$) or near-prolate (for $\xi = 0.5$) configurations. For ξ in the range $0.3 - 0.5$, clouds with $\langle q \rangle$ in the range $0.5 - 0.65$ have $\langle \Psi \rangle$ in the range $\simeq 10^\circ - 30^\circ$.

To illustrate the point that no single observation can establish the relative orientation of the field and the minor axis of the intrinsic three-dimensional object, we present in Figure 3 a view of a triaxial body with $(\xi, \zeta) = (0.3, 0.6)$ from three positions on the viewing sphere. This illustrates that all possible orientations of $B_\perp$ with the projected minor axis are possible, although the first panel shows the single most likely orientation and the middle panel is closest to the average orientation $\langle \Psi \rangle = 20^\circ$ for this case.

4. DISCUSSION

Our predicted probability distributions, with their correlation toward $\Psi = 0$, are in good agreement with early submillimeter polarimetry of dense regions. Matthews & Wilson (2000) measure three distinct regions in OMC-3, of which two imply near perfect alignment of $B_\perp$ with the projected minor axis, and one has $\Psi \gtrsim 30^\circ$. Ward-Thompson et al. (2000) infer $B_\perp$ in three dense cores, L1544, L183, and L43, and also find it to be correlated with the projected minor axes. They measure $\Psi = 29^\circ, 34^\circ$, and 44° for the three cores, respectively, although the last measurement is complicated by a nearby outflow and a weak polarization signal toward the core center. For L1544, the nonzero Ψ implies that the axisymmetric assumption in the magnetic model for that core developed by Ciolek & Basu (2000) needs to be relaxed, at least moderately. However, since that model does already account for flattening along the field lines, the magnetic field strength predictions would likely not change substantially.

Future large data sets of the offset angle Ψ, as submillimeter polarization measurements become common, will properly test the distributions of Ψ presented in this paper. Such data will provide a clear observational test between the scenario presented here (which is already supported by the Zeeman data), in which gravity and the mean magnetic field play an important role in shaping core structure (even in the presence of turbulence) and those scenarios in which turbulent compression is dominant, leading to the claim (Ballesteros-Paredes, Vazquez-Semadeni, & Scalo 1999) that there is no correlation between the magnetic field direction and the cloud elongation.

I thank the anonymous referee for comments which helped improve the paper. This research was supported by a grant from the Natural Sciences and Engineering Research Council of Canada.

[1]Such clouds are distinct from existing models of prolate clouds (Tomisaka 1991; Fiege & Pudritz 2000) in which the mean magnetic field lies along the major axis; here the mean field lies along the minor axis. The cloud can be prolate ($\zeta = \xi$) by chance, but there is no intrinsic symmetry that favors such a configuration, and the pressure exerted by the mean field makes it likely that $\zeta > \xi$ for most clouds.

REFERENCES

Ballesteros-Paredes, J., Vazquez-Semadeni, E., & Scalo, J. 1999, ApJ, 515, 286
Binney, J. 1985, MNRAS, 212, 767
Ciolek, G. E., & Basu, S. 2000, ApJ, 529, 925
Crutcher, R. M. 1999, ApJ, 520, 706 (C99)
Fiedler, R. A., & Mouschovias, T. Ch. 1993, ApJ, 415, 680
Fiege, J. D., & Pudritz, R. E. 2000, ApJ, 534, 291
Goodman, A. A., Bastien, P., Myers, P. C., & Ménard, F. 1990, ApJ, 359, 363
Goodman, A. A., Jones, T. J., Lada, E. A., & Myers, P. C. 1995, ApJ, 448, 748
Jijina, J., Myers, P. C., & Adams, F. C. 1999, ApJS, 125, 161
Langer, W. D. 1978, ApJ, 225, 95
Lin, C. C., Mestel, L., & Shu, F. H. ApJ, 142, 143
Lizano, S., & Shu, F. H. 1989, ApJ, 342, 834
Matthews, B. C., & Wilson, C. D. 2000, ApJ, 531, 868
Mestel, L. 1965, QJRAS, 6, 161
Mouschovias, T. Ch., 1976, ApJ, 207, 141
_____. 1978, in Protostars and Planets, ed. T. Gehrels (Tucson: Univ. Arizona Press), 209
_____. 1991, in The Physics of Star Formation and Early Stellar Evolution, ed. C. J. Lada and N. Kylafis, 449
Mouschovias, T. Ch., & Psaltis, D. 1995, ApJ, 444, L105
Myers, P. C., Fuller, G. A., Goodman, A. A., & Benson, P. J. 1991, ApJ, 376, 561
Myers, P. C., & Goodman, A. A. 1988, ApJ, 326 L27
Nakano, T., & Nakamura, T. 1978, PASJ, 30, 671
Schleuning, D. A. 1998, ApJ, 493, 811
Stark, A. A. 1977, ApJ, 213, 368
Tomisaka, K. 1991, ApJ, 376, 190
Vrba, F. J., Strom, S. E., & Strom, K. M. 1976, AJ, 81, 958
Ward-Thompson, D., Kirk, J. M., Crutcher, R. M., Greaves, J. S., Holland, W. S., & André, P. 2000, ApJ, 537, L135

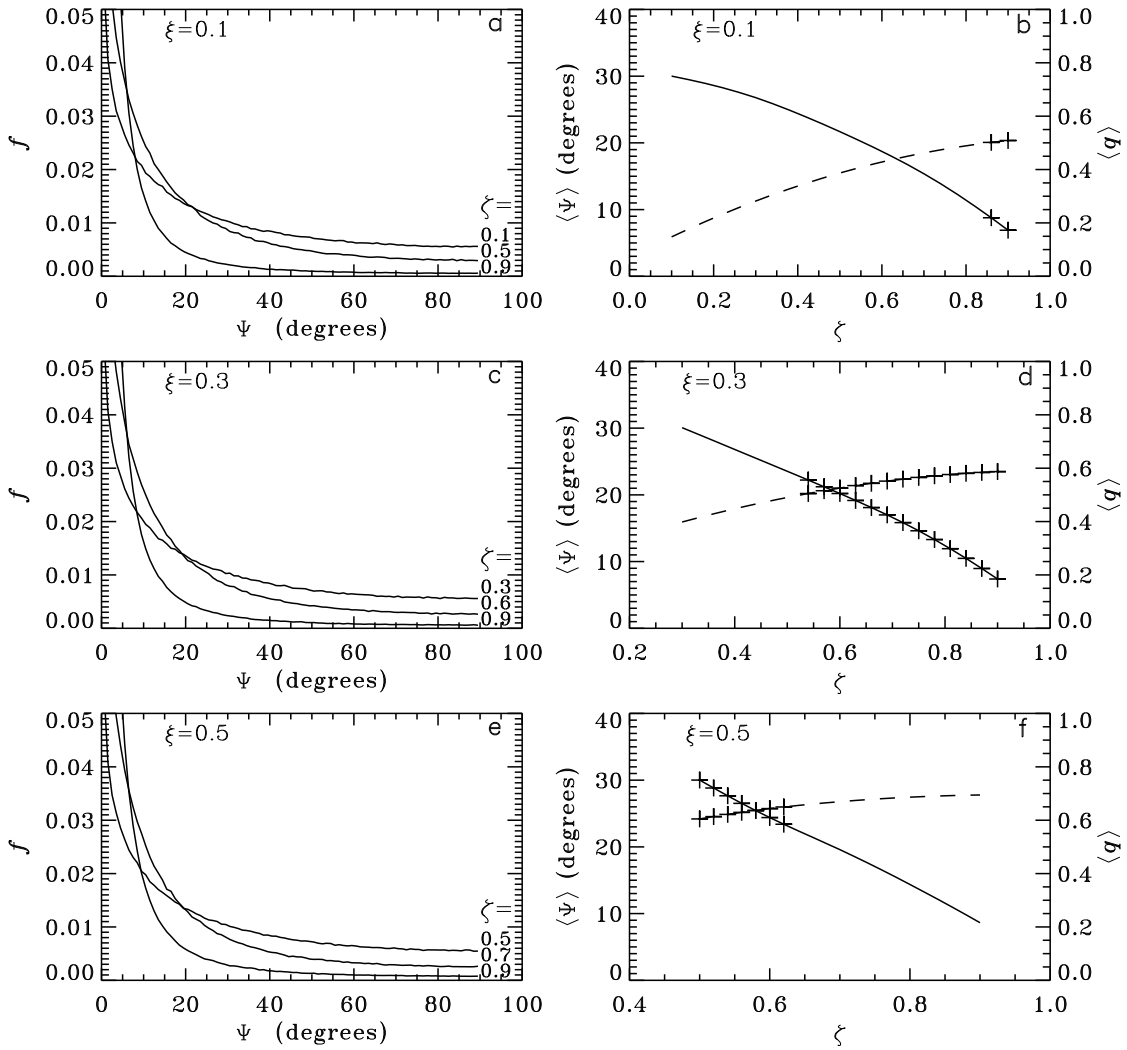

Fig. 2 Probability distribution function f versus angle Ψ for various values of (ξ, ζ), as well as the dependence of mean values $\langle\Psi\rangle$ and $\langle q\rangle$ on ζ for individual values of ξ. a) f versus Ψ for $\xi = 0.1$ and $\zeta = 0.1, 0.5, 0.9$. b) $\langle\Psi\rangle$ (solid line) and $\langle q\rangle$ (dashed line) versus ζ for $\xi = 0.1$. c) Same as a) but $\xi = 0.3$ and $\zeta = 0.3, 0.6, 0.9$. d) Same as b) but $\xi = 0.3$. e) Same as a) but $\xi = 0.5$ and $\zeta = 0.5, 0.7, 0.9$. f) Same as b) but $\xi = 0.5$. In b), d) and f), the crosses highlight the region in which $\langle q\rangle = 0.5 - 0.65$, consistent with observations.

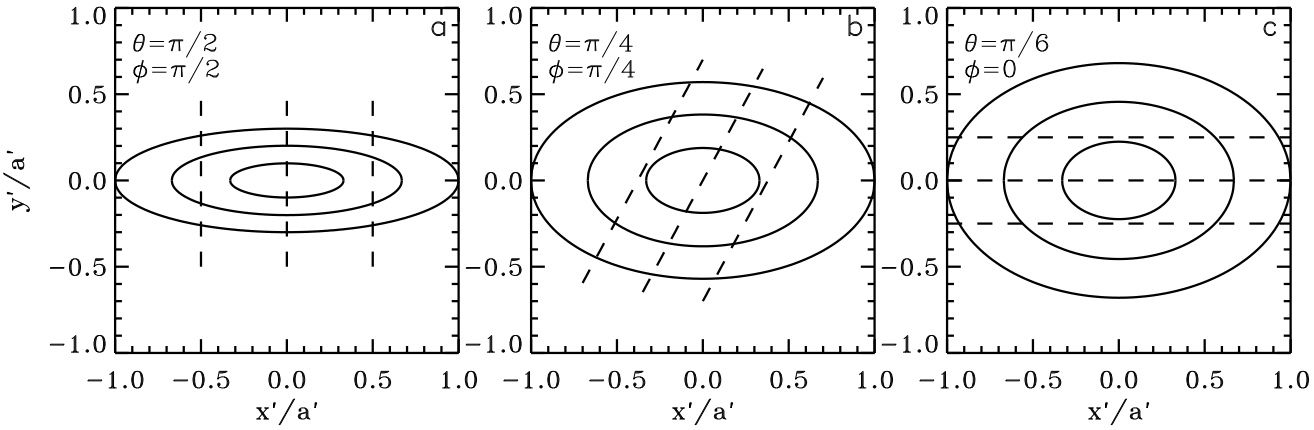

Fig. 3 Simulated contours (solid lines) and mean polarization direction (dashed lines) for a triaxial body with axial ratios $(\xi, \zeta) = (0.3, 0.6)$ seen from three sets of viewing angles (θ, ϕ). The The x' and y' axes are in the plane of the sky and are chosen to lie along the projected major and minor axes, and a' is the apparent semi-major axis. The dashed lines lie along the projected direction of the intrinsic z axis. a) $(\theta, \phi) = (\pi/2, 0)$, yielding an apparent axis ratio $q = 0.3$ and offset angle $\Psi = 0°$. b) $(\theta, \phi) = (\pi/4, \pi/4)$, yielding $q = 0.57$ and $\Psi = 28°$. c) $(\theta, \phi) = (\pi/6, 0)$, yielding $q = 0.68$ and $\Psi = 90°$.